Soft Matter

Fourier Transform Infrared Spectroscopy Investigation of Water Microenvironments in Polyelectrolyte Multilayers at Varying Temperatures

Journal:	*Soft Matter*
Manuscript ID	SM-ART-12-2019-002478.R1
Article Type:	Paper
Date Submitted by the Author:	31-Jan-2020
Complete List of Authors:	Eneh, Chikaodinaka; Texas A&M University College Station Bolen, Matthew; Texas A&M University College Station Suarez-Martinez, Pilar; Texas A&M University College Station Bachmann, Adam; North Carolina State University Zimudzi, Tawanda; Pennsylvania State University Hickner, Michael; Pennsylvania State University Batys, Piotr; Instytut Katalizy i Fizykochemii Powierzchni im. Jerzego Habera, Sammalkorpi, Maria; Aalto University Lutkenhaus, Jodie; Texas A&M University College Station

ARTICLE

Fourier Transform Infrared Spectroscopy Investigation of Water Microenvironments in Polyelectrolyte Multilayers at Varying Temperatures

Received 00th January 20xx,
Accepted 00th January 20xx

DOI: 10.1039/x0xx00000x

Chikaodinaka I. Eneh[a], Matthew J. Bolen[a], Pilar C. Suarez-Martinez[a], Adam Bachmann[b], Tawanda J. Zimudzi[c], Michael A. Hickner [c], Piotr Batys[d], Maria Sammalkorpi[e], Jodie L. Lutkenhaus*[af]

Polyelectrolyte multilayers (PEMs) are thin films formed by the alternating deposition of oppositely charged polyelectrolytes. Water plays an important role in influencing the physical properties of PEMs, as it can act both as a plasticizer and swelling agent. However, the way in which water molecules distribute around and hydrate ion pairs has not been fully quantified with respect to both temperature and ionic strength. Here, we examine the effects of temperature and ionic strength on the hydration microenvironments of fully immersed poly(diallyldimethylammonium)/ polystyrene sulfonate (PDADMA/PSS) PEMs. This is accomplished by tracking the OD stretch peak using attenuated total reflectance Fourier transform infrared (ATR-FTIR) spectroscopy at 0.25 M – 1.5 M NaCl and 35 – 70 °C. The OD stretch peak is deconvoluted into three peaks: 1) high frequency water, which represents a tightly bound microenvironment, 2) low frequency water, which represents a loosely bound microenvironment, and 3) bulk water. In general, the majority of water absorbed into the PEM exists in a bound state, with little-to-no bulk water observed. Increasing temperature slightly reduces the amount of absorbed water, while addition of salt increases the amount of absorbed water. Finally, a van't Hoff analysis is applied to estimate the enthalpy (11-22 kJ/mol) and entropy (48-79 kJ/molK) of water chaing from low to high frequency states.

Introduction

When positively and negatively charged polymers are brought together, they form solid-like complexes or liquid-like coacervates.(1-3) Complexation is driven by electrostatic attraction between negatively and positively charged polyelectrolytes (PE) and by entropic release of small counterions and water.(4-8) Similarly, complexation at a surface by the alternate deposition of polyanions and polycations results in polyelectrolyte multilayers (PEMs).(4, 9) The properties of PEMs are highly tunable and are dependent on polyelectrolyte type (strong or weak),(10) assembly techniques,(11, 12) pre-assembly and post-assembly conditions (pH, salt type and ionic strength, water content and relative humidity).(3, 13-15) PEMs have been examined for many applications including separations,(16, 17) electrochemistry,(18) anti-corrosion protection,(19) smart coatings(11, 20) and biosystems.(21) PEMs in the presence of water, salt solutions, solutions of varying pH, or solvents experience swelling or deswelling depending on a balance of hydrophobic/hydrophilic interactions and ion pairing.(2, 3, 22-27) Therefore, understanding the role of water within a PEM is important for manipulating swelling or deswelling of the PEM in its intended application.

Specifically, the response and swelling of PEMs consisting of poly(diallyldimethylammonium) (PDADMA) and poly(styrenesulfonate) (PSS) have been investigated using quartz crystal microbalance with dissipation monitoring (QCM-D),(3, 23, 28) nuclear magnetic resonance (NMR) spectroscopy,(29) ellipsometry,(30) atomic force microscopy (AFM),(30) and Fourier transform infrared (FTIR) spectroscopy.(31-33) QCM-D measurements indicated that the salt anion has a more pronounced influence on swelling than the cation.(3, 23, 28) Elsewhere, it was shown using NMR spectroscopy that positive surface charge leads to swelling, while a negative surface charge leads to deswelling.(29) From investigations using ellipsometry and AFM, Miller and Bruening(30) showed that PEMs containing polyelectrolytes with high charge density swell less due to a greater number of intrinsic (polycation-polyanion) ion pairs. Interestingly, PEM film thickness depended on the identity of the PEM's capping layer: for PDADMA/PSS multilayers, films capped with PDADMA swelled four times more than those with a PSS capping layer in the presence of water.(30) This behavior was attributed to the net positive charge of the PEM due to an excess of PDADMA in the PEM. Using IR-sensitive ions, attenuated total reflectance (ATR) FTIR spectroscopy has been employed to investigate

[a] Artie McFerrin Department of Chemical Engineering, Texas A&M University, College Station, Texas 77840, United States
[b] Department of Chemical and Biomolecular Engineering, North Carolina State University, Raleigh, North Carolina 27695, United States.
[c] Department of Materials Science and Engineering, The Pennsylvania State University, University Park, Pennsylvania 16802, United States
[d] Jerzy Haber Institute of Catalysis and Surface Chemistry, Polish Academy of Sciences, Niezapominajek 8, PL-30239 Krakow, Poland
[e] Department of Chemistry and Materials Science, Aalto University, P.O. Box 16100, 00076 Aalto, Finland
[f] Department of Materials Science and Engineering, Texas A&M University, College Station, Texas 77840, United States

cation uptake in PDADMA/PSS films upon exposure to ionic liquids.(33) These findings include PEM hydration and swelling reversibility.

Polyelectrolyte complexes (PECs) have been described as brittle when dry and "leathery and rubbery" when wet,(34) which emphasizes the importance of properly identifying the water content and determining the role of water molecules within the complex phase. Reports exist that detail the bulk effect of water on PECs and PEMs in terms of swelling, morphology, and mechanical properties.(22, 29, 30, 35, 36) However, although attempts have been made to study the microstructural level role of water within PECs,(31, 37) an understanding of the distribution, binding, and dynamics of water molecules at varying post-assembly environments, and connection of these to materials characteristics, remains lacking.

A previous study(37) applied a combination of molecular dynamics (MD) simulations and differential scanning calorimetry (DSC) to distinguish among different states of freezing and non-freezing bound water surrounding the charged groups within the PEC at hydration levels as high as 30 wt%. However, that investigation was not able to access the case for fully immersed or fully hydrated PECs.

Elsewhere, Schlenoff *et al.*(31) performed ATR-FTIR spectroscopy measurements to quantify the amount of water and its distribution around intrinsic vs extrinsic ion pairs in PEMs. It was observed that at lower NaCl concentrations (<0.5 M), water was withdrawn from the PEM but at higher concentrations (0.5 – 2.0 M), the PEMs swelled. Schlenoff *et al.* also investigated the *in situ* build-up of PDADMA/PSS films prepared at varying ionic strengths and polyelectrolyte stoichiometry using ATR-FTIR spectroscopy to explore the relationship between water and the glass transition temperature (T_g).(38) Investigation of the two overlapping modes of the OH stretch region of water (3244 and 3412 cm^{-1}) showed that the populations represented by these modes were relatively constant, with respect to each other, over the explored temperature range (10 – 60 °C).(38) Also, the simultaneous decrease in the OH stretch peak and increase in the OD stretch peak upon the addition of HOD showed that all water molecules are replaceable within the PEM film.(38) While these prior studies have provided important insights into the water's location at intrinsic vs extrinsic ion pairs in PEMs, they did not quantify the nature of water's binding (tightly vs loosely bound), especially with respect to temperature.

Here, we examined the effect of both salt concentration and temperature on the distribution of water in PDADMA/PSS PEMs using ATR-FTIR spectroscopy. The PDADMA/PSS system was selected for this study because it is a well-studied system with known properties.(1-3, 7, 22, 26, 27, 29, 30, 38, 39) 70 layer-pairs of PDADMA/PSS were prepared on a ZnSe substrate in the presence of 0.5 M NaCl to yield a PEM dry thickness of 2.5 µm. For these assembly conditions, the PEM is expected to consist of 35 – 36 mol% PSS.(3) In a flow-through ATR-FTIR cell, the as-made films were then exposed to aqueous solutions of varying NaCl concentration (0.25 M – 1.5 M) and the temperature was varied from 35 to 70 °C. These temperatures are well-above the T_g of each immersed, fully-hydrated PEM.(40) PDADMA/PSS complexes deconstruct at NaCl concentrations greater than 2.5 M,(1, 15) so the films are expected to remain stable over this range of ionic strength. Deuterated water, HOD (initially 5 v% D_2O in H_2O), was utilized to quantify the response. The OD stretch peak was deconvoluted to represent three water micro-environments: high frequency, low frequency, and bulk water. High frequency water describes water that is tightly-bound to the polyelectrolyte ion pairs, low frequency water is loosely-bound to the polyelectrolyte ion pairs, and bulk water is considered to be unassociated to the material. The deconvoluted peak areas and positions are interpreted in the context of how water's microenvironment within the multilayer evolves with temperature and ionic strength. The results are also discussed within the larger context of multilayer swelling, annealing, and self-healing.

Materials and Methods

Materials

Poly(diallyldimethylammonium) (PDADMA, M_w = 200,000 - 350,000 g/mol, 20 wt% solution) and polystyrene sulfonate (PSS, M_w = 500,000 g/mol) were purchased from Polysciences, Inc. Deuterium oxide (D_2O) (99.8% deuterium) was purchased from Tokyo Chemical Industries Co. and sodium chloride (NaCl) was purchased from Sigma-Aldrich. A 45° angle zinc selenide (ZnSe) crystal purchased from Specac Ltd.

Solution Preparation

Each PDADMA and PSS aqueous solution was prepared at a concentration of 1 g/L. For assembly, the salt concentration of both polyelectrolyte solutions and rinsing solutions was 0.5 M NaCl. An HOD mixture was prepared using 5 v% D_2O (4.52 mol% D_2O) with 95% Milli-Q deionized H_2O and various NaCl concentrations for ATR-FTIR measurements.

Layer-by-Layer (LbL) Assembly

The ZnSe crystal substrate was cleaned using Milli-Q water, then acetone, followed by air-drying to remove any residual solvent. LbL assembly of the polyelectrolytes was performed using an automated HMS slide stainer from Carl Zeiss, Inc. at room temperature. The ZnSe crystal was placed in a basket with the surface to be tested exposed. One layer of PDADMA on the ZnSe crystal was made by immersing the crystal in 1 g/L PDADMA solution for 15 min, followed by three rinses in 0.5 M NaCl with agitation for 2 min, 1 min, and 1 min. Similarly, a layer of PSS was deposited by repeating the same sequence. These two steps comprise a "layer pair", and the process was repeated to deposit 70 layer-pairs. The dry thickness of a 70 layer-pair PDADMA/PSS film, measured using a profilometer (KLA Tencor D-100), was determined to be 2.5 µm. Thus, 70 layer-pair films were prepared for all measurements to ensure that the film thickness was greater than the ZnSe penetration depth of the ATR-FTIR evanescent wave (0.71 – 0.80 µm for 2400 - 2700 cm^{-1}).(41) The expected refractive index of these 70-layer pair films decreases with increased hydration and lies between 1.45 and 1.5.(23, 42) PEM films were dried in ambient conditions overnight.

ATR-FTIR Spectroscopy

ATR-FTIR spectroscopy was performed using a Nicolet 6700 FTIR spectrometer from Thermo Scientific. A ZnSe crystal background spectrum was taken on a clean crystal under nitrogen purge over a temperature range of 35 - 70 °C, increasing by 5 °C increments to assess the effect of temperature on background spectra. The background spectra were independent of temperature, thus the background spectrum at 35 °C was chosen as the representative reference spectrum for all subsequent experiments (**Figure S1**). Each spectrum was recorded with a resolution of 4 cm^{-1} with 32 scans over the range of 400 - 4000 cm^{-1}. To examine the response of a PEM at very low hydration as a control, ATR-FTIR spectroscopy was performed on each PEM using 100 µL of varying concentrations of NaCl HOD pipetted onto the FTIR stage (**Figure S2**). Following the same procedure, measurements were performed over the same temperature range on each PEM fully immersed in ~850 µL of NaCl HOD solutions. Experiments were carried out in triplicate. We observed batch-to-batch variation in the absolute absorbance values, but the location of the peaks and the trends with salt and temperature were internally consistent.

FTIR Spectral Analysis

All spectra were processed using Omnic software and were baselined by fixing the absorbance at the end points of the wavelength region (400 - 4000 cm^{-1}). **Figure 1a** shows a sample deconvoluted FTIR spectrum between 2400-2700 cm^{-1} obtained for PDADMA/PSS PEMs immersed in 0.5 M NaCl HOD at 35 °C. Because of our two-point baselining routine, very low absorbance regions of the spectrum can give slightly negative responses. This could be mitigated by a multi-point baselining strategy, but this type of baselining can introduce other types of errors. Thus, we chose the simplest, most repeatable baselining routine. The small negative values in the spectrum do not influence our results since that portion of the examined region is small. The examined range represents the OD asymmetrical stretch peak and the spectrum was deconvoluted to show the following water microenvironments : the low and high frequency vibrational bands are attributed to water molecules in different hydrogen-bonding environments. The high frequency component corresponds effectively to stronger PE-water interactions (weaker hydrogen bonds) and the low frequency components to weaker PE-water interactions (stronger hydrogen bonds).(43) Therefore, the water molecules with high frequency OD stretching can be identified as strongly bound to the polyelectrolyte. All OD peaks were corrected for non-Condon effects(44) (**Figure S3**) and analyzed using a previously published three-population deconvolution method(45) with Origin 8.0 Pro. These three peaks are here-in called the bulk water peak, the low frequency (loosely bound water) peak, and the high frequency (tightly bound water) peak.

First, the low and high frequency peak shapes were determined by examining a PEM under low hydration conditions; a three-peak fit was performed by fixing the bulk water peak center and full width half max (FWHM) (2509 cm^{-1} and 170 cm^{-1}, respectively)(46, 47) while allowing the other peak shapes (peak center and FWHM) to vary. For fully immersed samples, the bulk water peak intensity was then unconstrained, while fixing the high frequency peak shape (center and FWHM) and the low frequency peak center. The low frequency peak's FWHM was left unconstrained because as hydration increases, the low frequency peak's FWHM will potentially change due to a broadening of the distribution of states within this population.(48) The fits were iterated until their cumulative sum of the least squares difference was minimized. In examining all of the data, the deconvolutions were essentially reduced to two peak fittings due to the very small contribution from the bulk water peak. **Figure 1b** provides a visual representation of the high and low frequency water surrounding the polyelectrolyte ion pairs in the presence of salt ions. High frequency water is strongly bound to the polyelectrolyte ion pairs while low frequency, loosely bound, water maintains interactions with the polyelectrolyte or resides in outer hydration shells. Bulk water (if observed) would exist in

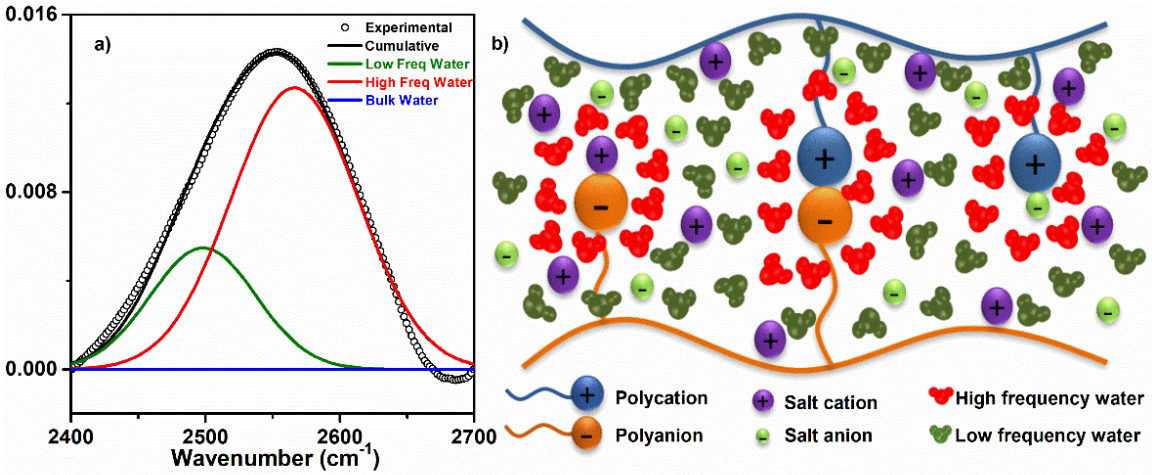

Figure 1 (a) A sample spectrum showing deconvolution of the OD asymmetrical stretching region from 2400 to 2700 cm^{-1} of PDADMA/PSS PEM immersed in 0.50 M NaCl HOD solution. The three peaks (in blue, green, and red) correspond to populations of HOD in different states of association within the surrounding environment: bulk water, low frequency water, and high frequency water. (b) A visual representation of the water microenvironments and their distribution around both intrinsic and extrinsic ion pairs showing low frequency and high frequency water.

regions where the water molecules have no influence from the polyelectrolyte ion pairs.

Results and Discussion

In general, the uptake of water swells the PEM; specifically, a 4-layer pair of PDADMA/PSS capped with PDADMA prepared in 090Schlenoff and Dubas showed that PDADMA/PSS films prepared in the presence of 1.0 M NaCl swell up to 2.03 times that of the dry thickness when immersed in pure water.(22) However, the films had a lower swelling ratio when immersed in < 0.7 M NaCl solutions, and higher ratios when immersed in > 0.7 M NaCl.(22) Similarly, a decrease in thickness or no change was observed in PDADMA/PSS films (assembled from 0.5 M NaCl) when exposed to 0.1 M (~5% thickness decrease) and 0.5 M (~0% thickness change) KBr post assembly whereas films exposed to KBr solutions of lower or higher concentrations experienced swelling.(3) These works show that PDADMA/PSS PEMs may swell or slightly contract depending on the doping salt concentration, the capping layer, and assembly conditions.

Figure 2a shows FTIR spectra over the range of 400 - 4000 cm^{-1} for a film immersed in 0.5 M NaCl HOD. **Figure 2b and 2c**, which show in detail the OH and OD stretching peaks, reveal a decrease in peak area as temperature increases up to 70 °C, indicating a reduced amount of water present in the films. Also, as temperature increased, a shift in the peak position from 2524 cm^{-1} to 2535 cm^{-1} was observed in the OD stretch peak shown in **Figure 2c**. This peak shift to higher wavenumber is indicative of a decrease in hydrogen bonding amongst the water molecules as temperature increases and a change to more tightly bound water.(46) For example, water in the form of ice has its OD stretch peak center at 2440 cm^{-1} but in the form of water vapor, the peak center is at 2719 cm^{-1}.(49) The data presented in both **Figures 2b and 2c** reflect the qualitative shift of low frequency water populations to higher frequencies and also that water uptake into the multilayers is reduced with temperature.

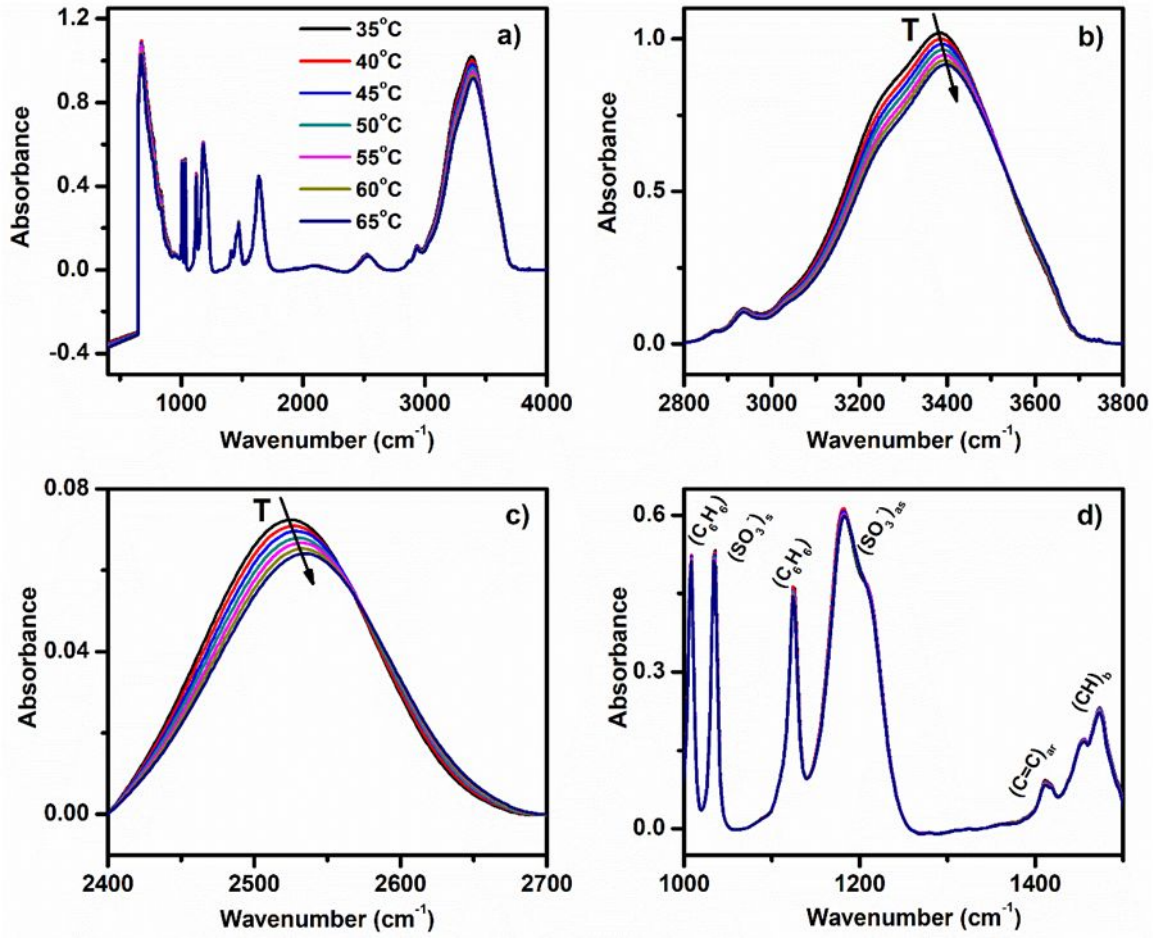

Figure 2: a) Set of baselined FTIR spectra for a 70-layer pair PDADMA/PSS film assembled in 0.50 M NaCl solution and immersed in 0.50 M NaCl HOD solution at different temperatures; Expanded view of b) the OH stretching region (2800 - 3800 cm^{-1}), c) the OD stretching region (2400 - 2700 cm^{-1}) and d) the polymer finger print region (1000 - 1500 cm^{-1}).

Figure 2d presents the fingerprint region showing characteristic peaks at 1007, 1034, 1124, 1191, 1419 and 1472 cm^{-1}. The peak at 1472 cm^{-1} is assigned to the contribution due to bending of the CH bond from PDADMA and the peak at 1419 cm^{-1} is assigned to the C=C rocking contribution of PSS.(33) Symmetric and anti-symmetric vibrations of the SO_3^- group appear as the 1034 and 1191 cm^{-1} peaks, respectively.(5, 33, 50) Peaks at 1007 and 1124 cm^{-1} are assigned to the in-plane vibration and in-plane bending vibration of benzene ring.(50, 51) **Figure 2d** shows that there was no change in the fingerprint region spectra with increasing temperature. This result enables the deduction that the amount of polyelectrolyte molecules present in the multilayer is not affected by the temperature variations.

However, the introduction of counterions into the PEMs post-assembly causes variations in the sulfonate anti-symmetric stretch peak (**Figure S4** and **S5**). In brief, the sulfonate anti-symmetric peak increases in area with the addition of salt up to 0.75 M NaCl, and then decreases in area with higher ionic strengths. This is attributed to polyelectrolyte and anti-polyelectrolyte effects,(52) as well as the increased formation of extrinsic ion pairs via screening effects.(3) An increase in peak area is observed as NaCl concentration increased to 0.75 M. This can be explained by an increase in PE-counterion pairing upon addition of salt, leading to tighter packed assemblies. Above 0.75 M, the PEMs experience swelling due to electrostatic screening effects leading to a drop in peak area.

Taking into consideration the difficulties associated with analyzing OH stretch peaks, which have overlapping bands,(53) the OD stretch peak instead was used to study water interactions in PDADMA/PSS multilayer systems. The deconvolution of the OD stretch peak of the multilayer immersed in 0.25 M NaCl HOD solution at 35 – 70 °C is shown in **Figure 3**. Previous work suggests that the peak positions of the high and low frequency peaks change with properties of the polymer, but the bulk water characteristics stay constant.(48) However, only two peaks are visible in **Figure 3**, attributed to low and high frequency water; the absence of a bulk water peak indicates that there is little or no bulk water present in the PEMs. This lack of bulk water may be due to the low porosity within the PEMs, which suggests that water molecules are always within the influence of the polyelectrolyte ionic groups.

Likewise, a study using modulated differential scanning calorimetry (MDSC) showed the absence of bulk water in PDADMA/PSS PECs at hydration levels of 18 to 30 wt%.(37) This indicates that the water content in the PEC either existed totally as non-freezing bound water or with a small fraction of freezing bound, water which was identified at 30% hydration.(37) Consistent with these findings, the absence of a bulk water peak from a deconvoluted OD peak was attributed to the high density of the ionic groups for homopolymer sulfonated poly(styrene).(48)

Figure 3 shows that as the temperature increases the high frequency water peak center shifts from 2553 to 2566 cm^{-1} (15 cm^{-1} shift toward effectively more tightly bound water), but a nearly constant peak area is maintained (the high frequency peak area increases by only 1.0 % with increasing temperature).

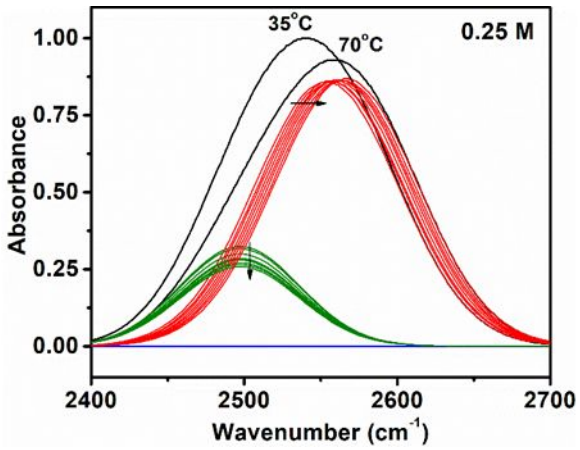

Figure 3: Deconvolutions of OD stretch peak for a PDAMA/PSS PEM immersed in 0.25 M NaCl HOD with arrows indicating the change in peak position as temperature increased from 35 °C to 70 °C. High frequency water (red), low frequency water (green), bulk water (blue) and cumulative water (black) peaks are shown. Similar deconvolutions for other salt concentrations are presented in Figure S6 (see Supporting Information). Spectra are corrected for non-Condon effects.

The lower frequency loosely bound water peak maintains its center at 2497 ± 0.01 cm^{-1}, while the peak area decreases by 20 %.

In general, the FTIR spectral peak position shifts and area changes with temperature can be directly explained via increasing thermal energy of water molecules in the system. Especially for the strongly bound water molecules, the translational and rotational motion is restricted, which results in increased vibrational motion.(37) The thermal motions at higher temperatures also lead to effectively weaker hydrogen bonding by the water molecules.(49) However, in our data the tightly bound high frequency water peak shifts towards higher wavenumber which suggests that the PE-water associations are getting effectively stronger (hydrogen bonding strength decreases) with increasing temperature. This may seem counterintuitive, considering the fact that temperature, in general, should presumptively weaken the hydrogen bonds between PE and water.(54) However, the reduction in cumulative water peak area means that the system is losing water which leads to a decrease in the overall electrostatic screening of water and consequently effectively stronger bonding to the material for the tightly bound water molecules.

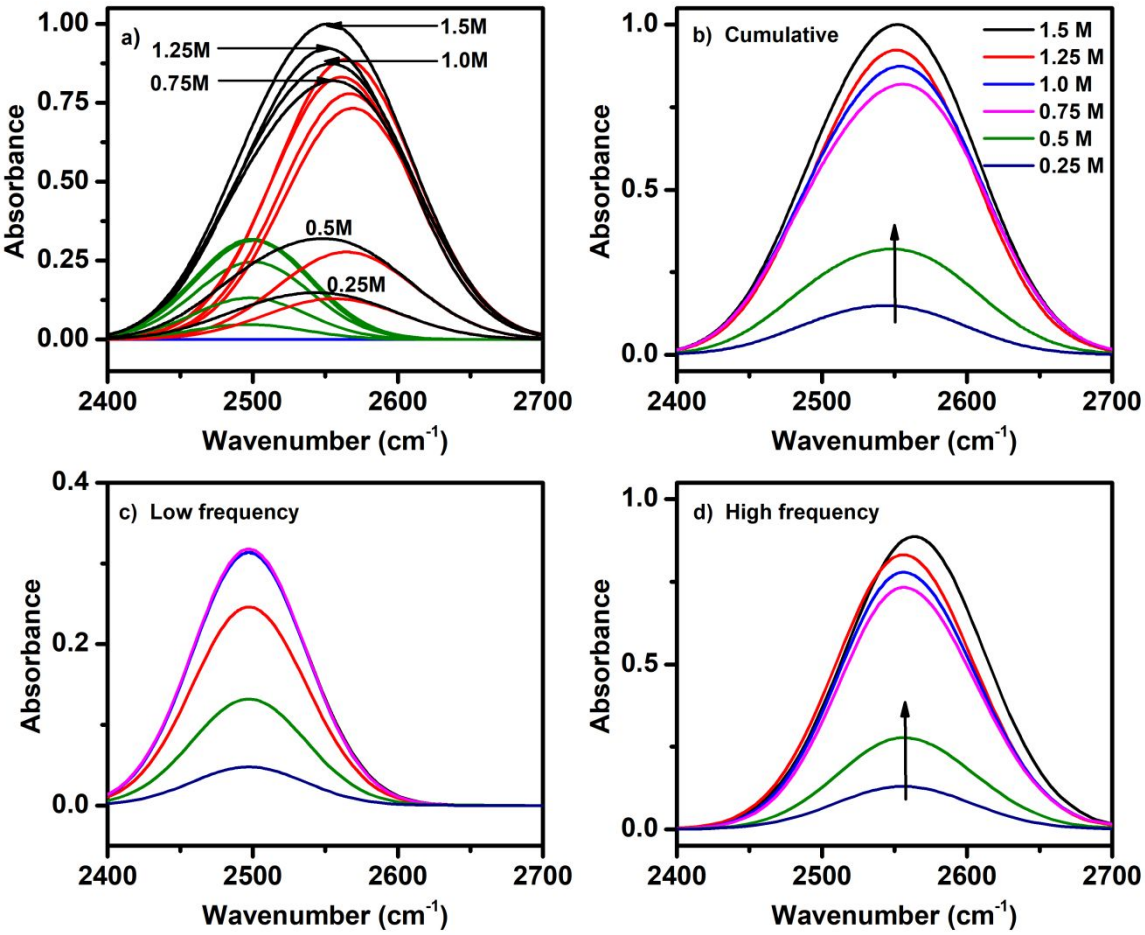

Figure 4: a) Combined deconvolutions for a PEM immersed in HOD solutions of different salt concentrations at 40 °C showing the cumulative (black), high (red) and low frequency water (green), and bulk water (blue) peaks. b) Cumulative c) Low frequency d) High frequency water peaks at different salt concentrations at 40 °C obtained from Figure 4a for clarity. The arrows in (b) and (d) indicate the trend with increasing salt concentration.

Throughout the examined temperature range, the high frequency water peak maintained a constant peak area in **Figure 3**. This data indicates that a constant number of water molecules constitutes the high frequency water at all temperatures in the system. We suggest that all ion pairs are fully surrounded by high frequency water at all examined conditions with no change in hydration as temperature is varied. This potentially suggests that at extremely low hydrations all added water may exist as high frequency water, tightly bound to the ionic groups and hydrating them. Once the maximum amount of high frequency water is absorbed into the PEM, additional water becomes low frequency, loosely bound water and eventually bulk water. An earlier simulation work shows the saturation response of tightly bound water upon increasing hydration in partially hydrated PDADMA/PSS complexes. (37, 54)

However, contrary to the tightly bound high frequency water, the weakly bound low frequency water exists with a fixed effective hydrogen bonding energy: its peak center remained constant at 2497 ± 0.01 cm^{-1}, while the peak area decreased with increasing temperature. The decrease of the low frequency peak area with temperature suggests that the absolute amount of weakly bound water molecules decreases. At the microscopic level, this is very likely related with breaking some of the weaker hydrogen bonds in the outer hydration shell, which leads to release of water molecules, perhaps into the external contacting solution. At the macroscopic level, this would indicate that, as temperature increases, the PEMs hold less water.

The results presented in **Figure 3** can be used to complement the interpretation of previous MD simulation results on partially hydrated PDADMA-PSS PECs(37) to provide some additional insight to the behavior of water molecules in this system. As the FTIR spectral characterization of this work was done for fully hydrated and immersed systems, we restrict the consideration to the temperature response. Both the data in **Figure 3** and previous reports(37) suggest that most of the water in the PEM is strongly bound even at high water content. **Figure 3**, moreover, indicates that strongly bound water dominates also in fully hydrated PDADMAC/PSS systems.

Figure 4 compares the deconvolution of OD stretch peaks for varying salt concentrations of NaCl in HOD at a constant temperature of 40 °C. While the peak area of all the cumulative OD stretch peaks generally increased with increasing NaCl concentration, the cumulative peak center at all concentrations remained approximately constant. The deconvolution of the

cumulative OD peak also shows that the areas of the high and low frequency water peaks increased with the addition of salt (**Figure 4 c-d**). These results indicate the PEMs swell with water as the ionic strength of the contacting solution increases. This finding is in accordance with previous studies of PDADMA/PSS multilayers in the presence of KBr using QCM-D,(3) where the swelling response showed different regions of response as a function of the salt concentration of the contacting solution. The origin of this behavior has two features: an increase in ionic strength 1) breaks intrinsic polycation-polyanion pairs, allowing for an increase in free volume of the PEM network and 2) presumably causes swelleing due to incoming water molecules that are hydrating the absorbed salt ions. This can be expected to lead to varying degrees of swelling of the multilayer, and previous simulation works also show that the presence of ions influences the water structure and PE-PE binding.(39, 55, 56). In addition to examining the changes in peak area, we also sought to inspect changes in peak center; however, the peak center shifts were very subtle and within the resolution of the instrument (~4 cm^{-1}).

A possible explanation for these variations may be related to the dual nature of salt in polyelectrolyte assemblies.(39) Salt ions act as plasticizer to the PEMs by bringing additional water molecules, which is clearly demonstrated by the increasing peak area in **Figure 4**. On the other hand, salt ions strongly bind water molecules through hydration of the ions and, therefore, compete with the polyelectrolytes for water interactions. At higher salt concentration, this effect can be pronounced enough to influence the hydration shell around polyelectrolytes by altering the number of water molecules or qby altering the polyelectrolyte-water binding strength. As suggested by molecular dynamics simulations for the PDADMAC/PSS system,(39) the increase in salt concentration decreases the amount of water around PSS and simultaneously increases the PSS-water hydrogen bond strength (or hydrogen bond lifetime). The increase in binding strength, as mentioned above, may be manifested by the shift in the high frequency peak center towards higher values. As can be seen in **Table S1**, at a constant temperature, a slight shift in high frequency peak center with increasing salt concentration can be observed. Altogether, our results combined with previous considerations,(3, 39) suggest that salt is changing the nature of polyelectrolyte-water binding.

Figure 5 demonstrates a comparison of the effects of temperature and salt concentration on the population distribution of water within the PDAMA/PSS PEM. **Figure 5a** shows the variation of high frequency and low frequency OD peak areas with temperature at different NaCl concentrations. The results show that about 80% of water molecules contribute to the high-frequency peak and are more tightly bound; also, the relative peak area percentages do not change much with regard to temperature. **Figure 5b** compares the effects of salt concentration for two different temperatures, 40 and 65 °C, on the population distribution of water within the PDADMA/PSS PEM. Similarly, there is little variation in the relative contributions of the high and low frequency peaks with regard to salt concentration. At 40 °C, the relative contribution of high

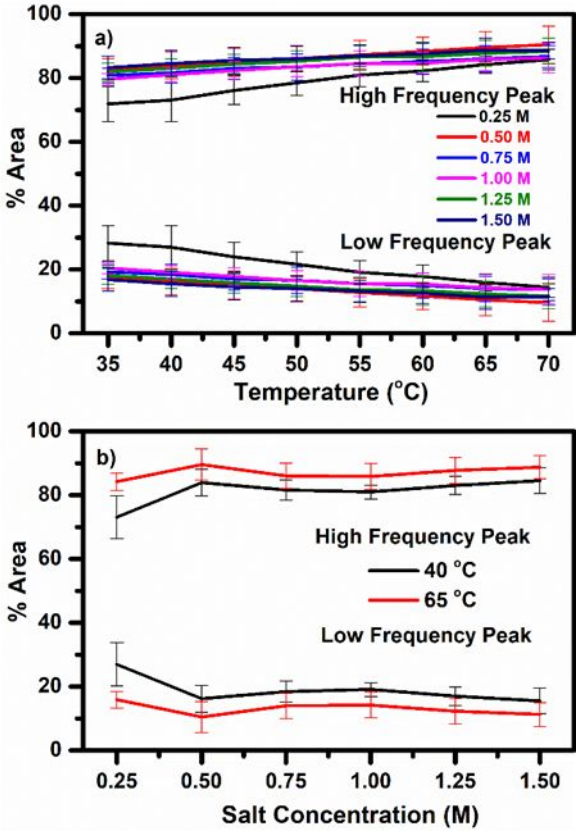

Figure 5: (a) Population distribution of water as percent area of each state for all tested salt concentrations and temperatures. (b) Comparison of percent area of low and high frequency peaks with respect to increasing salt concentration at 40 °C (black) and 60 °C (red). The two top-most (higher percentage) lines correspond to the high frequency water peaks and the two bottom-most (lower percentage) correspond to the low frequency water peaks.

frequency water is slightly reduced, but remains within error of the contribution at 65 °C.

To obtain more insight into the temperature response of water within the PEMs, a van't Hoff plot was constructed, **Figure 6**. The plot is based on the high and low frequency water populations from the deconvolution of OD stretch peaks and shows the natural logarithm of the ratio of the high frequency to low frequency water population against the inverse of temperature for each salt concentration of PEM. This analysis considers the equilibrium "reaction" of low frequency water shifting its state to high frequency water, Eqn 1. Assuming that the equilibrium of the reaction may be represented as the ratio of the high frequency water concentration to the low frequency water concentration, we can represent the van't Hoff equation as Eqn 2. Further assuming that each water population is proportional to its respective FTIR peak area, the van't Hoff equation may be modified to Eqn 3. This relationship predicts that the slope and y-intercept of the van't Hoff plot will yield the enthalpy and entropy of the conversion of low frequency water to high frequency water.(57)

$$H_2O|_L \leftrightarrow H_2O|_H \qquad \text{Eqn 1}$$

$$K_{eq} = \frac{[H_2O|_H]}{[H_2O|_L]} = \frac{A_H}{A_L} \qquad \text{Eqn 2}$$

$$\ln K_{eq} = \ln \frac{A_H}{A_L} = -\frac{\Delta H}{RT} + \frac{\Delta S}{R} \qquad \text{Eqn 3}$$

the ionic groups. Increasing the salt concentration led to the disruption of intrinsic polycation-polyanion pairs, which led to swelling of the film, as evidenced by the relative increase in the OD stretch peak area. The high and low frequency peak areas were quantified, and the peak area ratio followed a van't Hoff-

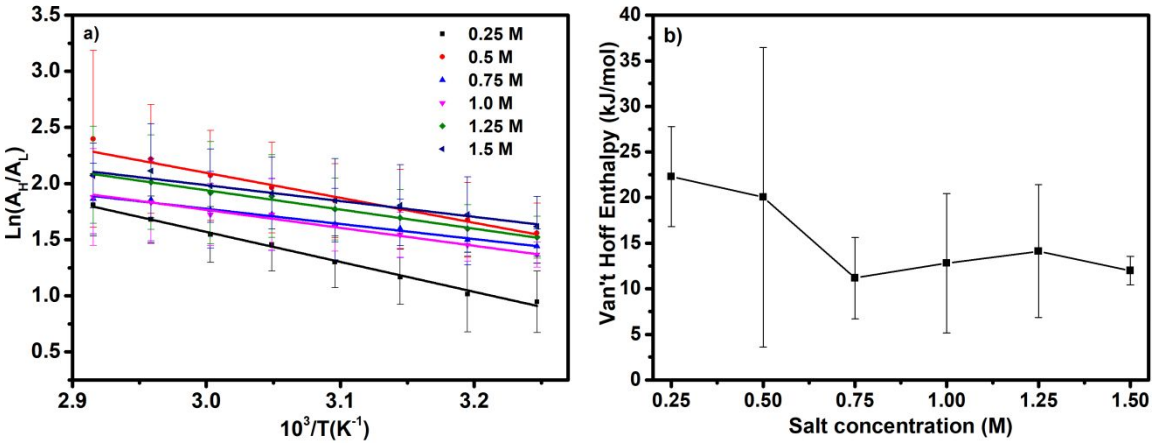

Figure 6: a) van't Hoff plot produced using the percent areas from Figure 5. The lines represent linear fits using the van't Hoff relationship. b) van't Hoff enthalpy dependence on salt concentration

In accordance with typical van't Hoff behavior, the data present a linear trend of ln (A_H/A_L) ~ 1/T. The linear trend suggests that the enthalpy and entropy are independent of temperature for the experiment. Notably in **Figure 6a**, the data sets corresponding to 0.25 M and 0.5 M have the greatest slopes. This means that, for these data sets, the ratio of the high frequency peak area to low frequency peak area is most sensitive to temperature change. In practice, the peak area change occurs mostly for the low frequency water peak but not so much for the high frequency peak. This means that these intermediate salt concentrations are more sensitive to the release of weakly bound water with increasing temperature. **Figure 6b,** shows that the calculated van't Hoff enthalpy values range from 11 – 22 kJ/mol (2.6 – 5.2 kcal/mol) across the different salt concentrations studied. Similarly, the van't Hoff entropy values range from 48 – 79 kJ/molK (11.5 – 19) kcal/molK). Using various techniques including Raman and IR spectroscopy, light and neutron scattering, and molecular dynamics, the van't Hoff enthalpy of liquid water has been obtained within the range from 2.3 – 3 kcal/mol,(58) which is of similar value here.

Conclusions

The influence of salt concentration and temperature on the hydrogen bonding of water molecules (specifically, HOD molecules) within PDADMA/PSS films was studied via ATR-FTIR spectroscopy. Deconvolution of OD stretch peak led to the conclusion that most of the water molecules in a fully hydrated PEM are located within regions of influence with the polymers (tightly or loosely bound), regardless of salt concentration or temperature. An increase in temperature caused an overall decrease in the amount of water within the film, but the amount of tightly bound water remained constant, indicating that water was released only from the outer hydration shells of type relationship. The van't Hoff enthalpy was in the range of 11 – 22 kJ/mol, which is in accordance with a typical hydrogen bonding response.

Altogether in this study, we showed that the water content in fully hydrated PEMs is influenced both by salt concentration and temperature, while the binding and interactions nature of individual polyelectrolyte molecules in the multilayers are controlled mostly by the salt counterions. Temperature plays a role via thermal vibrations, but it was not observed to change the binding character of the polyelectrolytes. An assessment of the distribution of water binding around the ion pairs was also made. Microenvironments of water molecules with high and low effective hydrogen bonding energy were identified; the amount of high frequency water remained relatively constant with temperature and salt indicating consistent hydration of the tightly bound water species in the PEM; meanwhile, the amount of low frequency water decreased with temperature indicating a loss of some of the more weakly hydrogen bonded water molecules with increasing temperature. The results provide insight into the character of water in PEMs but also lay foundation to understanding the varied microenvironments of water molecules within any charged system, whether it be synthetic or biological.

Conflicts of interest

There are no conflicts to declare

Acknowledgements

This work is supported by the National Science Foundation under Grant No. 1609696 (J. L. L.), Academy of Finland Grant No. 309324 (M. S.), and National Science Centre (Poland) Research Grant Sonata, UMO 2018/31/D/ST5/01866 (P. B). M.S.

is grateful for the support by the FinnCERES Materials Bioeconomy Ecosystem.

References

1. Zhang Y, Yildirim E, Antila HS, Valenzuela LD, Sammalkorpi M, Lutkenhaus JL. The influence of ionic strength and mixing ratio on the colloidal stability of PDAC/PSS polyelectrolyte complexes. Soft Matter. 2015;11(37):7392-401.
2. Parveen N, Schönhoff M. Swelling and Stability of Polyelectrolyte Multilayers in Ionic Liquid Solutions. Macromolecules. 2013;46(19):7880-8.
3. O'Neal JT, Dai EY, Zhang Y, Clark KB, Wilcox KG, George IM, et al. QCM-D Investigation of Swelling Behavior of Layer-by-Layer Thin Films upon Exposure to Monovalent Ions. Langmuir. 2018;34(3):999-1009.
4. Decher G, Hong JD, Schmitt J. Buildup of ultrathin multilayer films by a self-assembly process: III. Consecutively alternating adsorption of anionic and cationic polyelectrolytes on charged surfaces. Thin Solid Films. 1992;210-211:831-5.
5. Farhat T, Yassin G, Dubas ST, Schlenoff JB. Water and Ion Pairing in Polyelectrolyte Multilayers. Langmuir. 1999;15(20):6621-3.
6. v. Klitzing R. Internal structure of polyelectrolyte multilayer assemblies. Physical Chemistry Chemical Physics. 2006;8(43):5012-33.
7. Dubas ST, Farhat TR, Schlenoff JB. Multiple membranes from "true" polyelectrolyte multilayers. Journal of the American Chemical Society. 2001;123(22):5368-9.
8. Decher G. Fuzzy Nanoassemblies: Toward Layered Polymeric Multicomposites. Science. 1997;277(5330):1232-7.
9. Richardson JJ, Cui J, Björnmalm M, Braunger JA, Ejima H, Caruso F. Innovation in Layer-by-Layer Assembly. Chemical Reviews. 2016;116(23):14828-67.
10. Choi J, Rubner MF. Influence of the Degree of Ionization on Weak Polyelectrolyte Multilayer Assembly. Macromolecules. 2005;38(1):116-24.
11. Richardson JJ, Björnmalm M, Caruso F. Technology-driven layer-by-layer assembly of nanofilms. Science. 2015;348(6233):aaa2491.
12. Izquierdo A, Ono SS, Voegel JC, Schaaf P, Decher G. Dipping versus Spraying: Exploring the Deposition Conditions for Speeding Up Layer-by-Layer Assembly. Langmuir. 2005;21(16):7558-67.
13. Dubas ST, Schlenoff JB. Polyelectrolyte Multilayers Containing a Weak Polyacid: Construction and Deconstruction. Macromolecules. 2001;34(11):3736-40.
14. Abu-Sharkh B. Stability and structure of polyelectrolyte multilayers deposited from salt free solutions. The Journal of Chemical Physics. 2005;123(11):114907.
15. Dubas ST, Schlenoff JB. Factors Controlling the Growth of Polyelectrolyte Multilayers. Macromolecules. 1999;32(24):8153-60.
16. Sahadevan R, Yan Y, Chang H-C, Gao H, Phillip W. Mixed Mosaic Membranes Prepared by Layer-by-Layer Assembly for Ionic Separations. ACS nano. 2014;8.
17. Yang L, Tang C, Ahmad M, Yaroshchuk A, Bruening ML. High Selectivities among Monovalent Cations in Dialysis through Cation-Exchange Membranes Coated with Polyelectrolyte Multilayers. ACS Applied Materials & Interfaces. 2018;10(50):44134-43.
18. Pappa A-M, Inal S, Roy K, Zhang Y, Pitsalidis C, Hama A, et al. Polyelectrolyte Layer-by-Layer Assembly on Organic Electrochemical Transistors. ACS Applied Materials & Interfaces. 2017;9(12):10427-34.
19. Suarez-Martinez PC, Robinson J, An H, Nahas RC, Cinoman D, Lutkenhaus JL. Polymer-clay nanocomposite coatings as efficient, environment-friendly surface pretreatments for aluminum alloy 2024-T3. Electrochimica Acta. 2018;260:73-81.
20. Borges J, Mano JF. Molecular Interactions Driving the Layer-by-Layer Assembly of Multilayers. Chemical Reviews. 2014;114(18):8883-942.
21. Izumrudov VA, Mussabayeva BK, Murzagulova KB. Polyelectrolyte multilayers: preparation and applications. Russian Chemical Reviews. 2018;87(2):192-200.
22. Dubas ST, Schlenoff JB. Swelling and Smoothing of Polyelectrolyte Multilayers by Salt. Langmuir. 2001;17(25):7725-7.
23. Guzmán E, Ritacco H, Rubio JEF, Rubio RG, Ortega F. Salt-induced changes in the growth of polyelectrolyte layers of poly(diallyl-dimethylammonium chloride) and poly(4-styrene sulfonate of sodium). Soft Matter. 2009;5(10):2130-42.
24. Gao C, Leporatti S, Moya S, Donath E, Moehwald H. Swelling and Shrinking of Polyelectrolyte Microcapsules in Response to Changes in Temperature and Ionic Strength. Chemistry (Weinheim an der Bergstrasse, Germany). 2003;9:915-20.
25. Köhler K, Biesheuvel M, Weinkamer R, Moehwald H, Sukhorukov G. Salt-Induced Swelling-to-Shrinking Transition in Polyelectrolyte Multilayer Capsules. Physical review letters. 2006;97:188301.
26. Dodoo S, Steitz R, Laschewsky A, von Klitzing R. Effect of ionic strength and type of ions on the structure of water swollen polyelectrolyte multilayers. Physical Chemistry Chemical Physics. 2011;13(21):10318-25.
27. Reid DK, Summers A, O'Neal J, Kavarthapu AV, Lutkenhaus JL. Swelling and Thermal Transitions of Polyelectrolyte Multilayers in the Presence of Divalent Ions. Macromolecules. 2016;49(16):5921-30.
28. Han L, Mao Z, Wuliyasu H, Wu J, Gong X, Yang Y, et al. Modulating the Structure and Properties of Poly(sodium 4-styrenesulfonate)/Poly(diallyldimethylammonium chloride) Multilayers with Concentrated Salt Solutions. Langmuir. 2012;28(1):193-9.
29. Schwarz B, Schönhoff M. Surface Potential Driven Swelling of Polyelectrolyte Multilayers. Langmuir. 2002;18(8):2964-6.
30. Miller MD, Bruening ML. Correlation of the Swelling and Permeability of Polyelectrolyte Multilayer Films. Chemistry of Materials. 2005;17(21):5375-81.
31. Schlenoff JB, Rmaile AH, Bucur CB. Hydration Contributions to Association in Polyelectrolyte Multilayers and Complexes: Visualizing Hydrophobicity. Journal of the American Chemical Society. 2008;130(41):13589-97.
32. Jaber JA, Schlenoff JB. Counterions and Water in Polyelectrolyte Multilayers: A Tale of Two Polycations. Langmuir. 2007;23(2):896-901.
33. Parveen N, Schönhoff M. Quantifying and controlling the cation uptake upon hydrated ionic liquid-induced swelling of polyelectrolyte multilayers. Soft Matter. 2017;13(10):1988-97.
34. Michaels AS. POLYELECTROLYTE COMPLEXES. Industrial & Engineering Chemistry. 1965;57(10):32-40.
35. Yildirim E, Zhang Y, Lutkenhaus JL, Sammalkorpi M. Thermal Transitions in Polyelectrolyte Assemblies Occur via a Dehydration Mechanism. ACS Macro Letters. 2015;4(9):1017-21.
36. Zhang Y, Li F, Valenzuela LD, Sammalkorpi M, Lutkenhaus JL. Effect of Water on the Thermal Transition Observed in Poly(allylamine hydrochloride)–Poly(acrylic acid) Complexes. Macromolecules. 2016;49(19):7563-70.
37. Batys P, Zhang Y, Lutkenhaus JL, Sammalkorpi M. Hydration and Temperature Response of Water Mobility in

Poly(diallyldimethylammonium)–Poly(sodium 4-styrenesulfonate) Complexes. Macromolecules. 2018;51(20):8268-77.
38. Fu J, Abbett RL, Fares HM, Schlenoff JB. Water and the Glass Transition Temperature in a Polyelectrolyte Complex. ACS Macro Letters. 2017;6(10):1114-8.
39. Zhang R, Zhang Y, Antila HS, Lutkenhaus JL, Sammalkorpi M. Role of Salt and Water in the Plasticization of PDAC/PSS Polyelectrolyte Assemblies. The Journal of Physical Chemistry B. 2017;121(1):322-33.
40. Zhang Y, Batys P, O'Neal JT, Li F, Sammalkorpi M, Lutkenhaus JL. Molecular Origin of the Glass Transition in Polyelectrolyte Assemblies. ACS Central Science. 2018;4(5):638-44.
41. Minnes R, Nissinmann M, Maizels Y, Gerlitz G, Katzir A, Raichlin Y. Using Attenuated Total Reflection–Fourier Transform Infra-Red (ATR-FTIR) spectroscopy to distinguish between melanoma cells with a different metastatic potential. Scientific Reports. 2017;7(1):4381.
42. Löhmann O, Zerball M, von Klitzing R. Water Uptake of Polyelectrolyte Multilayers Including Water Condensation in Voids. Langmuir. 2018;34(38):11518-25.
43. Kitadai N, Sawai T, Tonoue R, Nakashima S, Katsura M, Fukushi K. Effects of Ions on the OH Stretching Band of Water as Revealed by ATR-IR Spectroscopy. Journal of Solution Chemistry. 2014;43(6):1055-77.
44. Black SB, Chang Y, Bae C, Hickner MA. FTIR Characterization of Water–Polymer Interactions in Superacid Polymers. The Journal of Physical Chemistry B. 2013;117(50):16266-74.
45. Smedley SB, Zimudzi TJ, Chang Y, Bae C, Hickner MA. Spectroscopic Characterization of Sulfonate Charge Density in Ion-Containing Polymers. The Journal of Physical Chemistry B. 2017;121(51):11504-10.
46. Moilanen DE, Piletic IR, Fayer MD. Tracking Water's Response to Structural Changes in Nafion Membranes. The Journal of Physical Chemistry A. 2006;110(29):9084-8.
47. Park S, Fayer MD. Hydrogen bond dynamics in aqueous NaBr solutions. Proc Natl Acad Sci U S A. 2007;104(43):16731-8.
48. Smedley SB, Chang Y, Bae C, Hickner MA. Measuring water hydrogen bonding distributions in proton exchange membranes using linear Fourier Transform Infrared spectroscopy. Solid State Ionics. 2015;275:66-70.
49. Falk M, Ford TA. INFRARED SPECTRUM AND STRUCTURE OF LIQUID WATER. Canadian Journal of Chemistry. 1966;44(14):1699-707.
50. Yang JC, Jablonsky MJ, Mays JW. NMR and FT-IR studies of sulfonated styrene-based homopolymers and copolymers. Polymer. 2002;43(19):5125-32.
51. Wang Y, Shen Y, Zhang Y, Yue B, Wu C. pH-Sensitive Polyacrylic Acid (PAA) Hydrogels Trapped with Polysodium-p-Styrenesulfonate (PSS)2006. 563-71 p.
52. Wang F, Yang J, Zhao J. Understanding anti-polyelectrolyte behavior of a well-defined polyzwitterion at the single-chain level. Polymer International. 2015;64(8):999-1005.
53. Brubach J-B, Mermet A, Filabozzi A, Gerschel A, Roy P. Signatures of the hydrogen bonding in the infrared bands of water. The Journal of Chemical Physics. 2005;122(18):184509.
54. Batys P, Kivistö S, Lalwani SM, Lutkenhaus JL, Sammalkorpi M. Comparing water-mediated hydrogen-bonding in different polyelectrolyte complexes. Soft Matter. 2019;15(39):7823-31.
55. Antila HS, Sammalkorpi M. Polyelectrolyte Decomplexation via Addition of Salt: Charge Correlation Driven Zipper. The Journal of Physical Chemistry B. 2014;118(11):3226-34.
56. Antila HS, Härkönen M, Sammalkorpi M. Chemistry specificity of DNA–polycation complex salt response: a simulation study of DNA, polylysine and polyethyleneimine. Physical Chemistry Chemical Physics. 2015;17(7):5279-89.
57. Ninno A, Del Giudice E, Gamberale L, Congiu Castellano A. The Structure of Liquid Water Emerging from the Vibrational Spectroscopy: Interpretation with QED Theory2013.
58. Walrafen GE, Fisher MR, Hokmabadi MS, Yang WH. Temperature dependence of the low- and high-frequency Raman scattering from liquid water. The Journal of Chemical Physics. 1986;85(12):6970-82.

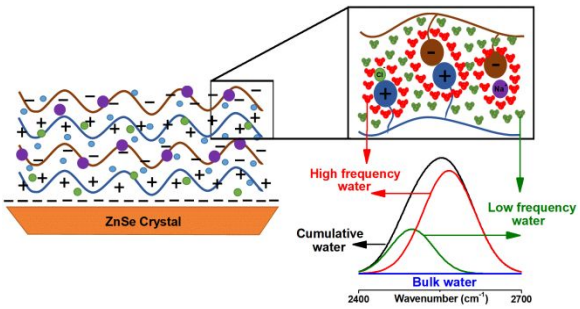

Tightly and loosely bound water molecules within polyelectrolyte multilayers are examined as a function of temperature and salt.